

Modeling and simulation of an Internal Combustion Engine using Hydrogen: A MATLAB implementation approach

Quang Truc Dam^{1,*} , Fatima Haidar¹ , Nour Mama¹ , Sherwin Joy Chennapalli¹ 

¹ Capgemini Engineering, Research & Innovation Direction, 12 rue de la Verrerie, 92190, Meudon, France

ABSTRACT

In response to the escalating global demand for energy spurred by industrialization, nations are increasingly turning to alternative fuel sources. Among these alternatives, hydrogen stands out for its remarkable efficiency and environmental benefits. With its potential to significantly reduce fuel consumption and air pollution, particularly in the transportation sector, hydrogen has garnered widespread attention as a promising solution to our energy challenges. This study focuses on the development of a dynamic model for an internal combustion engine powered by hydrogen (H₂-ICE). By intricately dissecting and modeling the various components of the engine and their interactions, we aim to create a comprehensive simulation platform. This platform will enable us to accurately predict and analyze the performance of H₂-ICE under different operating conditions. Through the utilization of advanced simulation tools like Matlab Simulink, we can validate the efficacy and reliability of our model, providing valuable insights into the behaviour of hydrogen-powered engines. Furthermore, the implications of this research extend beyond mere simulation. The developed model opens up avenues for further exploration and innovation in the field of hydrogen propulsion. For instance, it lays the groundwork for the development of sophisticated control systems tailored specifically for H₂-ICE applications. Additionally, the effectiveness of the proposed model in terms of air intake dynamics, pressure, temperature, fuel injection response, combustion efficiency, and overall engine performance, such as power output, torque, and engine velocity are illustrated through simulation results using Matlab Simulink.

Keywords: Automotive, Engine, Hydrogen, MATLAB - Simulink

History

Received: 04.03.2024

Accepted: 23.07.2024

Author Contacts

*Corresponding Author

e-mail addresses : Quang-truc.dam@capgemini.com , Fatima.haidar@capgemini.com .

Nour.mama@capgemini.com , Sherwin-joy.chennapalli@capgemini.com

How to cite this paper:

Dam, Q.T., Haidar, F., Mama, N., Chennapalli, S.J., (2024). Modeling and simulation of an Internal Combustion Engine using Hydrogen: A MATLAB implementation approach. Engineering Perspective, 4 (3), 108-118. <http://dx.doi.org/10.29228/eng.pers.76219>

1. Introduction

With the increase in the global population, energy demand is rising day by day. This not only depletes current energy reserves but also increases energy losses. Due to the limited potential of oil reserves, it is necessary to increase the use of alternative fuels. The use of hydrogen in combination with petroleum-derived fuels in internal combustion engines can reduce harmful exhaust emissions from fossil fuels. That is why researchers continue to work on an economical and safe fuel that does not harm the environment [1 - 5]. In addition to hydrogen-enriched petroleum fuels in internal combustion engines, various companies continue to work on fuel cells. One of the most important properties of hydrogen is that it does not harm the environment at the end of its combustion. With the development of

technology, the importance of hydrogen will increase for reasons such as increased production, cost reduction, and portability. Hydrogen is one of the important players in the clean energy sector. Hydrogen is a portable, storable, usable, and sustainable energy carrier in many different areas.

Over the past 30 years, extensive research has been conducted on the use of hydrogen as a fuel [6 - 8]. It is a directly usable energy source in the automotive sector with fuel cells. One of the most significant advantages of using hydrogen as a fuel in engines is that it reduces air pollution. Since there is no carbon in hydrogen fuel, there will be no emissions such as CO, CO₂, and HC at the end of combustion. When hydrogen energy is used in the transportation sector, which contributes to greenhouse effect, CO₂ emissions will be reduced. In a study conducted in Europe, it is estimated that by 2040,

new hydrogen vehicles will reduce CO₂ emissions by 35%, while hydrogen-powered public transport vehicles will reduce CO₂ emissions by 40%, with an average reduction in CO₂ emissions of 44.8 g/km [9].

Internal combustion engines are the most significant factors leading to an increase in environmental pollution [10 - 15]. The role of the internal combustion engine is to convert chemical energy into mechanical energy. In this engine, the system is renewed at each cycle. The system is in contact with only one heat source (the atmosphere and the fuel). Heat is produced by combustion in a variable volume chamber. It serves to increase the pressure within a gas filling this chamber (this gas is also initially composed of fuel and oxidizer: air). This increase in pressure results in a force exerted on a piston, a force that transforms the translational motion of the piston into the rotational motion of the shaft (crankshaft). The operation takes place in 4 stages: intake; compression; ignition (combustion); exhaust [11].

The most popular internal combustion engines are classified into two categories according to the ignition technique of the air-fuel mixture: spark ignition engines (gasoline engines) and compression ignition engines (Diesel engines).

A Diesel engine operates on the principle of self-ignition of the fuel. The richness of the mixture characterizes the engine load. The higher the load, the greater the quantity of injected fuel, while the airflow remains constant. When the piston rises in the combustion chamber (compression phase), it greatly increases the temperature and pressure, allowing the air-fuel mixture to self-ignite (the self-ignition potential of a fuel is characterized by the cetane number).

In a gasoline engine, the load is characterized by the airflow that varies depending on the load control. For an optimal compromise between performance, consumption, and emissions, gasoline engines operate around stoichiometry. Moreover, this promotes efficient operation of the three-way catalytic converter (for the three main pollutants: CO, NO_x, and HC). Indeed, the efficiency of this type of catalyst significantly degrades when deviating from stoichiometry.

Research indicates that most of the CO, HC, and NO_x compounds produced as a result of the combustion of fossil fuels come from gasoline and diesel engines. Harmful waste such as sulfur dioxide, lead, and soot are also present in the exhaust emissions of internal combustion engines [11], [16].

The sustainable use and production of hydrogen, which does not harm the environment, will be one possible solution. A hydrogen internal combustion engine vehicle is a type of hydrogen vehicle using an internal combustion engine. Hydrogen internal combustion engine vehicles are different from hydrogen fuel cell vehicles (which use hydrogen through electrochemical means rather than combustion). Instead, the hydrogen internal combustion engine is simply a modified version of the traditional gasoline internal combustion engine. Zero carbon means that no CO₂ is produced, thus eliminating the primary greenhouse gas emission from a conventional petroleum engine.

The characterization of an engine significantly affects its performance, leading to numerous studies aimed at optimizing engine performance. For instance, in [17], the surface of the combustion chamber is analyzed to understand heat transfer correlations. Similarly, the piston crown in relation to various combustion mode strategies

is investigated in [18]. The influence of fuel system variations on performance and emission characteristics is explored in [19], while [20] examines how combustion chamber geometry and fuel supply system variations can economize fuel consumption and reduce exhaust emissions. The impact of blended fuels with split injections on combustion and emission characteristics is analyzed in [21]. Additionally, [22] studies the effect of piston crown shape and the positioning of spark plugs and fuel injectors on fuel system control and emissions. Research in [23] delves into the use of hydrogen as a fuel for internal combustion engines, presenting a detailed analysis. Experimental studies focused on internal combustion engines fueled with hydrogen are also conducted in [24 - 25], offering valuable insights into the practical application and benefits of hydrogen as an alternative fuel. These comprehensive investigations collectively contribute to the advancement of engine design and fuel system optimization, highlighting the potential for improved efficiency and reduced environmental impact.

Motivated by the aforementioned studies, this research delves into the utilization of hydrogen as a fuel in an ICE, exploring a promising avenue towards reducing emissions and advancing sustainability in automotive propulsion systems. By leveraging the dynamic model initially developed for gasoline-powered ICEs, this study aims to adapt and extend it to accommodate the unique characteristics and operational parameters associated with hydrogen combustion. The goal is to construct a comprehensive and accurate dynamic model of an H₂-ICE, capable of simulating its performance under various operating conditions.

The proposed model facilitates further investigation into the effects of different components, including engine characterization, fuel characterization, and various methods of mixing fuel. For instance, by examining how hydrogen fuel impacts the combustion process, insights can be gained into optimizing fuel injection timing, air-fuel ratio, and ignition parameters to achieve efficient combustion and minimal emissions. Additionally, the model allows for the analysis of different hydrogen blending techniques and their effects on engine performance and emissions.

This study's dynamic model also provides a platform to explore the thermal management challenges unique to hydrogen combustion, such as its higher combustion temperature and faster flame speed compared to gasoline. Understanding these dynamics is crucial for designing effective cooling systems and ensuring engine durability. Moreover, the model can simulate the impact of hydrogen's lower energy density on fuel storage and delivery systems, offering insights into optimizing fuel tank design and refueling infrastructure for hydrogen-powered vehicles.

The effectiveness and fidelity of our proposed model will be rigorously assessed and validated using Matlab Simulink, a versatile platform widely employed for dynamic system modeling and simulation. Through meticulous calibration and validation against empirical data, we seek to ensure that our model accurately captures the dynamic behavior and performance nuances specific to hydrogen-fueled ICEs. This validation process is essential for establishing the reliability and predictive capability of our model, thus instilling confidence in its utility for subsequent analyses and optimization efforts.

2. Dynamic model of an H₂-ICE

Four-stroke internal combustion engines are the preferred choice

for conventional and hybrid vehicles due to their inherent fuel efficiency advantages over their two-stroke counterparts. This efficiency arises from the distinctive four-stroke engine cycle, where a power stroke occurs once every two revolutions of the crankshaft. This stands in contrast to two-stroke engines, which feature more frequent power strokes happening every revolution, resulting in higher fuel consumption per unit of power produced. Consequently, four-stroke engines boast reduced fuel consumption, emissions, and torque output compared to their two-stroke counterparts.

Key components of the four-stroke engine include the intake and exhaust manifold, intake and exhaust valves, spark plug, piston, coolant, cylinder, crankcase, connecting rod, and crankshaft. Each of these components plays a pivotal role in facilitating the engine's operation and performance. This study centers on the development of a comprehensive model for the four-stroke internal combustion engine, leveraging foundational research outlined in prior studies. Figure 1 provides a graphical representation of the fundamental operating principle of an internal combustion engine. It illustrates the sequential processes of intake, compression, power generation within the combustion chamber, and the subsequent transmission of torque to the crankshaft to drive the engine. Through meticulous modeling and analysis, this research aims to enhance our understanding of the intricate dynamics inherent to four-stroke engines, ultimately optimizing their performance in various automotive applications.

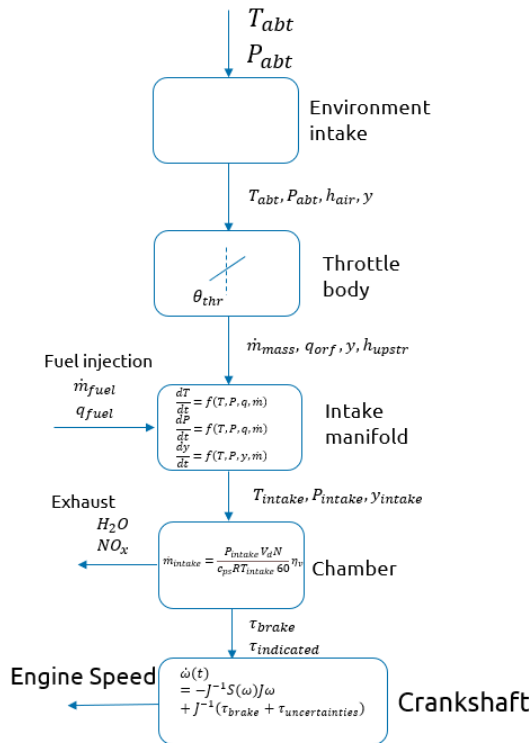


Figure 1. Representative operating diagram of the SI engine.

2.1. Intake Air System

The Intake Air System in an ICE is a crucial component responsible for delivering the appropriate amount of air to the engine's combustion chambers. Proper air intake is essential for efficient combustion and optimal engine performance. This system represents

the flow limit, which typically includes ambient temperature, pressure, specific enthalpy, and mass fraction (in the form of dry air). The ambient temperature and pressure (ambient temperature) can be constant or provided externally. The specific enthalpy is calculated as follows:

$$h_{air} = c_{p_{air}} T_{abt} \quad (1)$$

Where $c_{p_{air}}$ is the heat coefficient at constant and T_{abt} is the ambient temperature equal to 300K.

The mass fraction of dry air represents the percentage of different components in the inlet air, which are: Oxygen (O_2), Nitrogen (N_2), Unburned fuel (this component only appears after combustion), Carbon dioxide (CO_2), Water vapor (H_2O), Carbon monoxide (CO), Nitric oxide (NO), Nitrogen dioxide (NO_2), Nitric oxide and nitrogen dioxide (NO_x), Particulate matter, Air, Exhaust gases. Each component's mass fraction contributes to the overall composition of the inlet air, playing a crucial role in determining the system's behavior and performance characteristics.

2.2. Throttle Body

The throttle body is the part of the air intake system that controls the amount of air flowing into the engine, in response to driver accelerator pedal input in the main. The throttle body is usually located between the air filter box and the intake manifold, and it is usually attached to, or near, the mass airflow sensor. The mass flow rate through the throttle is determined as follow [16][26]:

The gas mass flow through the orifice:

$$\dot{m}_{orff} = \frac{A_{eff} P_{upstr}}{\sqrt{RT_{upstr}}} \Psi(P_{ratio}) \quad (2)$$

Where P_{ratio} is the ratio of downstream pressure (P_{dowstr}) and upstream pressure (P_{upstr}). $\Psi(P_{ratio})$

$$= \begin{cases} \sqrt{\gamma \left(\frac{2}{\gamma+1}\right)^{\frac{\gamma+1}{\gamma-1}}} & \text{if: } P_{ratio} < \left(\frac{2}{\gamma+1}\right)^{\frac{\gamma}{\gamma-1}} \\ \sqrt{\frac{2\gamma}{\gamma-1} \left(\frac{P_{ratio}^{\frac{2}{\gamma}}}{-P_{ratio}^{\frac{\gamma+1}{\gamma}}}\right)} & \text{if: } \left(\frac{2}{\gamma+1}\right)^{\frac{\gamma}{\gamma-1}} < P_{ratio} < P_{lim} \\ \frac{P_{ratio}-1}{P_{lim}-1} \sqrt{\frac{2\gamma}{\gamma-1} \left(\frac{P_{lim}^{\frac{2}{\gamma}}}{-P_{lim}^{\frac{\gamma+1}{\gamma}}}\right)} & \text{if: } P_{lim} < P_{ratio} \end{cases} \quad (3)$$

Where $P_{upstr} = P_{abt} = 101325$ Pa is the ambient pressure. $\Psi(P_{ratio})$ is the based follow correlation and is the function of P_{ratio} calculates the based on the different conditions of flow.

$$P_{ratio} = \frac{P_{dowstr}}{P_{upstr}} \quad (4)$$

Where P_{lim} is the pressure ratio limitation, $\gamma = 1.4$ is the ratio of specific heats. The air mass flow rate (\dot{m}_{air}) then can be calculated as follows:

$$\dot{m}_{air} = \dot{m}_{orff} \gamma_{upstr_air} \quad (5)$$

Where γ_{upstr_air} is the upstream species mass fraction.

A_{eff} is the effect area, and is calculated as follows:

$$A_{eff} = \frac{\pi}{4} D_{thr}^2 C_{thr}(\theta_{thr}) \quad (6)$$

$$\theta_{thr} = \theta_{ct_thr} \frac{90}{100} \quad (7)$$

Where θ_{thr} is the open angle of the throttle (in degree), θ_{ct_thr} is the percentage of throttle body that open, D_{thr} is the throttle diameter at opening, $C_{thr}(\theta_{thr})$ is the discharge coefficient.

The heat flow rate q_{orf} of is calculated as follows:

$$q_{orf} = \dot{m}_{orf} h_{upstr} \quad (8)$$

Where h_{upstr} is the upstream specific enthalpy (h_{air}).

2.3. Intake Manifold

To calculate the fuel flow in the hydrogen (H_2) internal combustion engine, one utilizes the characteristics of the fuel injector along with the fuel injector pulse-width. The model for fuel flow is expressed as:

$$\dot{m}_{fuel} = \frac{N S_{inj} P_{winj} N_{cyl}}{c_{ps} 1000 * 60} \quad (9)$$

Where N represents engine speed in rpm, S_{inj} denotes the fuel injector slope, N_{cyl} signifies the number of engine cylinders, c_{ps} stands for the crankshaft revolutions per power stroke.

The fuel heat flow rate is subsequently determined by:

$$q_{fuel} = \dot{m}_{fuel} h_{upstr} \quad (10)$$

In contrast to gasoline spark-ignition (SI) engines, where gasoline is the sole fuel, in the case of hydrogen (H_2) engines, the fuel also serves as the intake gas. Therefore, the intake gas mass flow rate and its associated fuel heat flow must be corrected. The corrected intake gas mass flow rate (\dot{m}_{in_intk}) is calculated as the sum of the fuel mass flow rate (\dot{m}_{fuel}) and the gas mass flow rate (\dot{m}_{gas}).

$$\dot{m}_{in_intk} = \dot{m}_{fuel} + \dot{m}_{gas} \quad (11)$$

Similarly, the corrected intake gas heat flow (q_{in_intk}) is determined by summing the fuel heat flow (q_{fuel}) and the gas heat flow (q_{orf}).

$$q_{in_intk} = q_{fuel} + q_{orf} \quad (12)$$

Subsequently, the species mass fractions are reformulated as follows:

$$y_{unbrn_fuel} = \frac{\dot{m}_{fuel}}{\dot{m}_{in_intk}} \quad (13)$$

$$y_{air} = \frac{\dot{m}_{gas}}{\dot{m}_{in_intk}} \quad (14)$$

$$y_{O_2} = 0.233 \frac{\dot{m}_{gas}}{\dot{m}_{in_intk}} \quad (15)$$

$$y_{N_2} = 0.767 \frac{\dot{m}_{gas}}{\dot{m}_{in_intk}} \quad (16)$$

In this study, the other mass fractions remain zero. These formulations allow for a comprehensive understanding of the fuel and gas flows within the hydrogen internal combustion engine, facilitating

accurate modeling and analysis of its performance characteristics. The intake manifold serves as a critical component of the air intake system, responsible for regulating the pressure and temperature of the air delivered to the cylinder. The changes in temperature and pressure within the intake manifold are dynamically determined by employing a constant volume chamber model containing an ideal gas. This analysis leverages the continuity equation and the first law of thermodynamics to accurately characterize the behavior of the intake manifold. The rate changes in temperature and pressure are determined by implementing a constant volume chamber containing an ideal gas, the continuity equation and the first law of thermodynamics is used in this case as follows:

$$\frac{dT_{intake}}{dt} = \frac{RT_{intake}}{c_{p,air} V_{ch} P_{intake}} \left((q_{in_intk} \right. \quad (17)$$

$$\left. - T_{intake} c_v \dot{m}_{in_intk} \right)$$

$$\left. - (q_{out_intk} \right.$$

$$\left. - T_{intake} c_v \dot{m}_{out_intk} \right))$$

$$\frac{dP_{intake}}{dt} = \frac{P_{intake}}{T_{intake}} \frac{dT_{intake}}{dt} \quad (18)$$

$$+ \frac{RT_{intake}}{V_{ch}} (\dot{m}_{in_intk} - \dot{m}_{out_intk})$$

Where R is Ideal gas constant, V_{ch} is Chamber volume, T_{intake} and P_{intake} are the chamber absolute temperature and pressure respectively, q_{out_intk} is the output heat flow given by Eq. 17, and \dot{m}_{out_intk} is the mass flow in the chamber given by Eq. 25. Hence the specific enthalpy of the intake manifold is calculated as:

$$h_{intake} = c_{p,air} T_{intake} \quad (19)$$

Using the conservation of mass for each gas constituent, the mass fraction of gas in the chamber can be determined as follows:

$$\frac{dy_{intake}}{dt} = \frac{RT_{intake}}{V_{ch} P_{intake}} \left((y_{in_intk} \dot{m}_{in_intk} \right. \quad (20)$$

$$\left. - y_{intake} \dot{m}_{out_intk} \right)$$

$$+ y_{intake} (\dot{m}_{in_intk} - \dot{m}_{out_intk}))$$

These equations provide a comprehensive framework for understanding the dynamic behavior of temperature, pressure, and gas composition within the intake manifold, facilitating accurate modeling and analysis for optimizing engine performance.

To determine the output heat flow (q_{out_intk}), we employ a heat transfer model depicted in Figure 2. This model accounts for both convective and conductive heat transfer processes occurring within the intake manifold. The output heat flow is calculated as the sum of convective ($Q_{1,conv}$) and conductive ($Q_{1,cond}$) heat transfer components.

$$q_{out_intk} = Q_1 = Q_{1,conv} = Q_{1,cond} \quad (21)$$

$$Q_2 = Q_{2,conv} = Q_{2,cond} \quad (22)$$

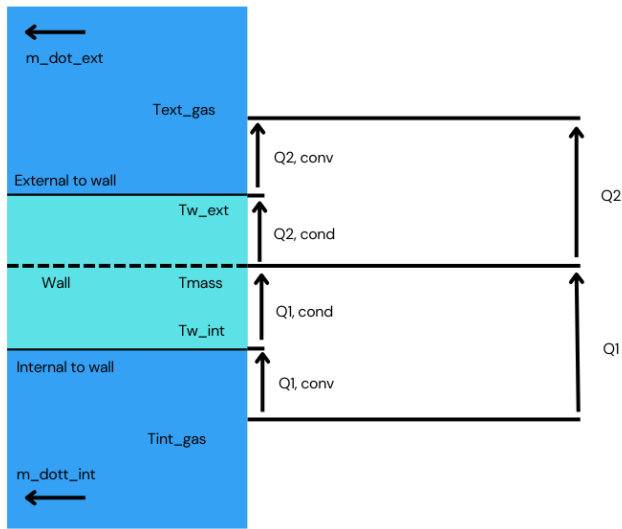


Figure 2. Heat transfer model

Firstly, $Q_{1,conv}$ represents the convective heat transfer from the intake gas to the interior wall of the manifold. It is computed using the equation:

$$Q_{1,conv} = c_{q,int}(\dot{m}_{in_intk})A_{int_conv}(T_{in_gas} - T_{w_int}) \quad (23)$$

Here, $c_{q,int}$ represents the convective heat transfer coefficient, \dot{m}_{in_intk} denotes the mass flow rate of the intake gas, A_{int_conv} is the convective surface area, T_{in_gas} is the temperature of the intake gas, and T_{w_int} represents the temperature of the interior wall of the intake manifold.

Secondly, $Q_{1,cond}$ denotes the conductive heat transfer from the interior wall of the manifold to the mass of the wall itself. It is given by:

$$Q_{1,cond} = \frac{k_{int}A_{int_cond}}{D_{int_cond}}(T_{w_int} - T_{mass}) \quad (24)$$

Where k_{int} is the thermal conductivity of the wall material, A_{int_cond} represents the conductive surface area, D_{int_cond} is the thickness of the wall, and T_{mass} denotes the temperature of the wall material.

Similarly, the heat transfer from the exterior wall of the manifold to the external environment is represented by $Q_{2,conv}$ and $Q_{2,cond}$. These components account for convective and conductive heat transfer processes, respectively, and are calculated using analogous equations, and are given as follows:

$$Q_{2,conv} = c_{q,ext}(ExtnlFlwVel)A_{ext_conv}(T_{w_ext} - T_{ext_gas}) \quad (25)$$

$$Q_{2,cond} = \frac{k_{ext}A_{ext_cond}}{D_{ext_cond}}(T_{mass} - T_{w_ext}) \quad (26)$$

Finally, the rate of change in temperature of the wall material

$(\frac{dT_{mass}}{dt})$ is determined by the difference between the input and output heat flows divided by the thermal capacity of the wall material as follows:

$$\frac{dT_{mass}}{dt} = \frac{Q_1 - Q_2}{c_{pwall}m_{wall}} \quad (27)$$

By incorporating Eq. (13) to Eq. (19) into this heat transfer model, we can accurately derive the output heat flow (q_{out_intk}), providing insights into the thermal dynamics of the intake manifold and facilitating optimization of heat management strategies for enhanced engine performance.

The Engine Cooling System serves several critical functions within the internal combustion engine (ICE) setup. Primarily, it acts to dissipate excess heat generated during engine operation, thereby preventing overheating and potential damage to engine components. Additionally, the cooling system plays a pivotal role in maintaining the engine at its optimal operating temperature, ensuring peak efficiency and performance. Furthermore, during engine startup, the cooling system facilitates the rapid attainment of the desired operating temperature, promoting smoother and more efficient engine operation from the outset.

In this study, our focus is not on designing the Engine Cooling System per se, but rather on integrating it seamlessly into our ICE system to form a closed-loop system. This integration is crucial for ensuring the overall functionality and efficiency of the ICE setup.

The temperature of the engine after undergoing the cooling process is governed by the following equation:

$$\frac{dT_{cooling}}{dt} = \frac{\dot{m}_{out_intk}(c_{p_air}T_{intake} - c_{p_air}T_{exh}) + LHV\dot{m}_{fuel} - \tau\omega}{c_{eng}} \quad (28)$$

Where LHV is the fuel lower heating value, ω is the engine speed in rad/s. $c_{eng} = 40000$ is the heat capacity.

The H₂-ICE model employed in this study is based on the Spark-Ignition (SI) engine model, with hydrogen (H₂) serving as a substitute for gasoline. This choice reflects a shift towards cleaner and more sustainable fuel alternatives, aligning with the broader objective of reducing emissions and promoting environmental sustainability in automotive applications.

By incorporating the Engine Cooling System into our H₂-ICE model, we can ensure the holistic simulation and analysis of the entire engine system, enabling comprehensive assessments of performance, efficiency, and thermal management strategies. This integrated approach lays the foundation for advancing the development and optimization of hydrogen-powered internal combustion engines for future automotive applications.

2.4. Air Mass Flow Model

To calculate the air mass flow in the engine chamber, one shall use a speed-density air mass flow model as depicted in Figure 3. The speed-density model uses the speed-density equation to calculate the engine air mass flow. The equation relates the engine air mass flow to the intake manifold gas pressure, intake manifold gas temperature, and engine speed. Consider using this air mass flow model in simple

conventional engine designs, where variable valvetrain technologies are not in use.

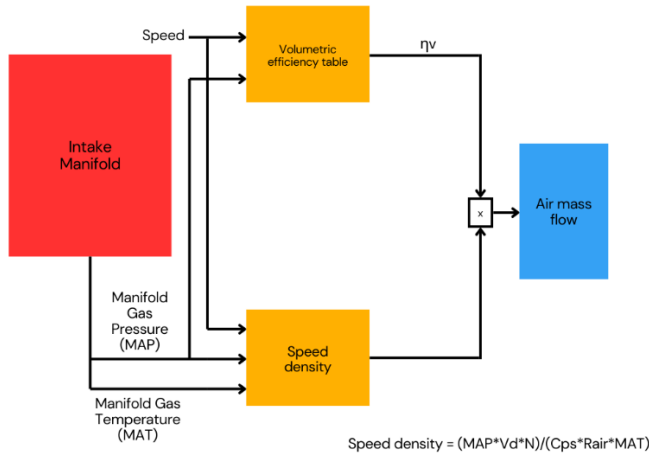


Figure 3. Engine Chamber Speed-Density Air Mass Flow Model

To determine the air mass flow, the speed-density air mass flow model applies these speed-density equations at the intake manifold gas pressure and gas temperature states.

The mass flow (\dot{m}_{intake}) at the intake port can be calculated as follows [16]-[26]:

$$\dot{m}_{intake} = \frac{P_{intake} V_d N}{c_{ps} R T_{intake} 60} \eta_v \quad (29)$$

Where η_v is engine volumetric efficiency as given in Figure 4, dimensionless, is a function of intake manifold absolute pressure (P_{intake}) and engine speed (N) and calculated as follows:

$$\eta_v = f(P_{intake}, N) = \dot{m}_{intake} \frac{c_{ps} R T_{intake} 60}{P_{intake} V_d N} \quad (30)$$

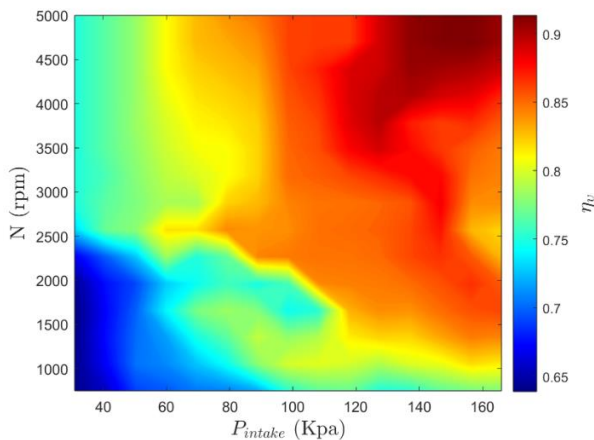


Figure 4. Engine volumetric efficiency

Subsequently, the calculated air mass flow is multiplied by the mass fraction of air (y_{intake_air}) in the intake mixture to determine the air mass (\dot{m}_{air_intake}):

$$\dot{m}_{air_intake} = y_{intake_air} \dot{m}_{intake} \quad (31)$$

Furthermore, the engine load (L_{eng}), a crucial parameter indicative of the engine's operational state, is derived using the formula:

$$L_{eng} = \frac{\dot{m}_{air_intake} c_{ps} * 60 R T_{std}}{V_d N P_{std}} \quad (32)$$

Where T_{std}, P_{std} are the standard temperature and pressure respectively.

The Air-Fuel ratio is calculated as:

$$ARF = \frac{\dot{m}_{air_intake}}{\dot{m}_{fuel}} \quad (33)$$

2.5. Torque Model

In the SI engine the indicated torque means that the torque or power of the engine is evaluated in the scope of thermodynamics (pressure and volume of cylinder), not including any mechanical losses in the whole power development and transmission process conceptually illustrates pressure variation in a cylinder along with crankshaft rotation angle. This torque is calculated as follows [11]:

$$\tau_{indicated} = \frac{P_{indicated} * 60}{2\pi N} \quad (34)$$

Where $P_{indicated}$ is the indicated power and can be calculated as:

$$P_{indicated} = \dot{m}_{fuel} * LHV \eta_{indicated} \quad (35)$$

Where $\eta_{indicated}$ is the engine indicated load efficiency as well as a function of engine speed (N) and indicated torque ($\tau_{indicated}$) as depicted in Figure 5.

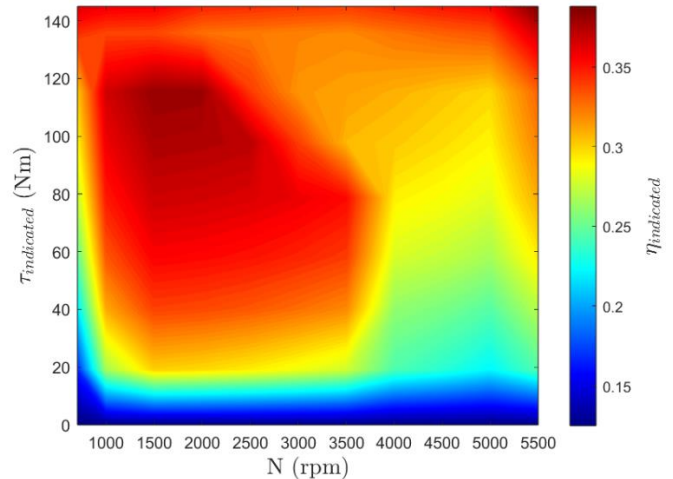


Figure 5. Indicated torque efficiency

Not all the torque produced in the cylinder (indicated power and torque) are available on the crankshaft. The available torque on the crankshaft is the difference between the indicated torque and friction torque, respectively, expressed as:

$$\tau_{brake} = \tau_{indicated} - \tau_{friction} \quad (36)$$

The basic engine accessories include a water pump, oil pump, fuel pump, and valve shaft. Other accessories may depend on applications, such as cooling fan, alternator, power steering pump, and air conditioner compressor. In an engine test, the accessories that are driven by the engine crankshaft should be clearly specified. All

power and torque requirements for driving accessories and overcoming frictions are grouped together and called the friction torque and is given as:

$$\tau_{friction} = \eta_{friction} f(L_{eng}, N) \tag{37}$$

where $\eta_{friction}$ is the friction temperature factor as demonstrated in Figure 7, $f(L_{eng}, N)$ is the function of engine load (L_{eng}) and engine speed (N) as depicted in Figure 6.

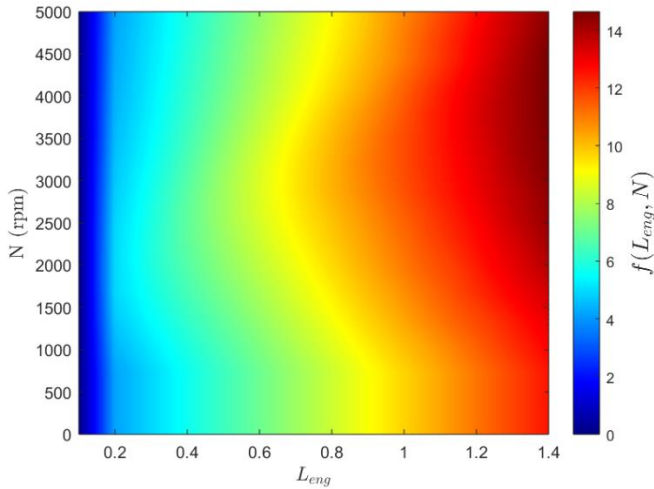


Figure 6. Friction force factor

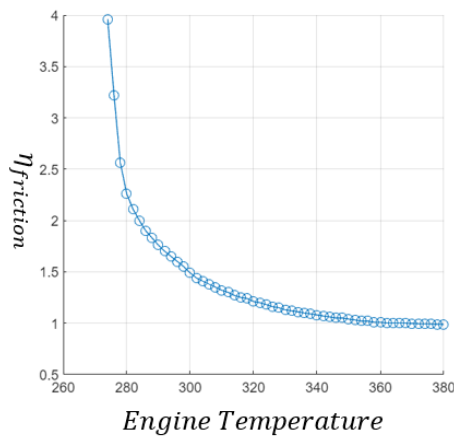


Figure 7. Friction temperature factor

3. Simulation Results and Discussion

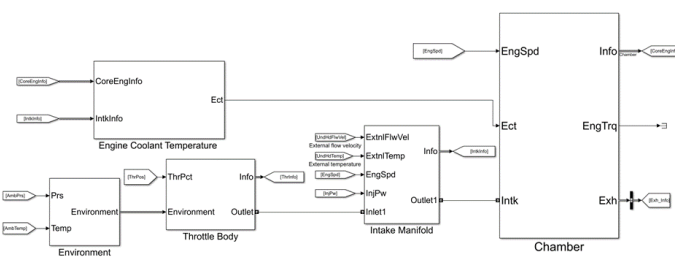


Figure 8. Detailed Simulink model for ICE

To illustrate the performance of the developed model, an explicative simulation will be conducted using Matlab Simulink, as shown in Figure 8. The simulation will utilize input references for the throttle valve open angle, given in Figure 9, and the fuel injector pulse-width, given in Figure 10, to demonstrate the model's performance. The scenario involves first regulating the throttle valve's open angle according to Figure 9, and then injecting hydrogen fuel into the engine following the values in Figure 10. This simulation aims to show how the throttle valve configuration affects overall system behavior, examining the relationship between throttle position and fuel injector pulse-width in controlling the air and fuel intake. Expected outcomes include insights into air intake dynamics, pressure, temperature, fuel injection response, combustion efficiency, and overall engine performance, such as power output, torque, and engine velocity. By integrating these findings, a comprehensive understanding of the throttle valve's influence on system behavior is achieved, providing a foundational step towards optimizing system design and enhancing operational efficiency. This detailed analysis ultimately validates the proposed H2-ICE model and offers valuable insights for further research and development in hydrogen-fueled automotive technologies.

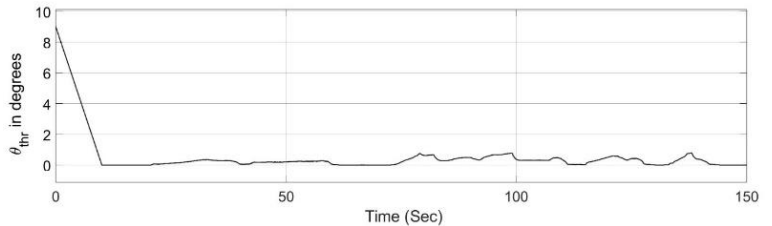


Figure 9. Throttle angle

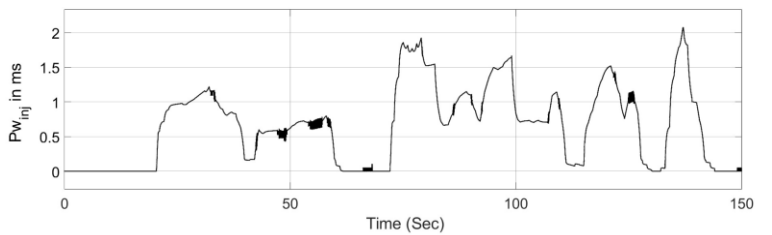


Figure 10. Fuel injector pulse-width

The ambient temperature and pressure are set up as 300 °K and 101325 Pa respectively, the Heat coefficient at constant $c_{p,air} = 1005 \text{ J/(kg}\cdot\text{K)}$. We consider the dry air contains only oxygen and nitrogen with its mass fraction are given as $y_{O_2} = 0.233$ and $y_{N_2} = 0.767$.

The downstream pressure within the intake manifold is calculated by applying Eq. (18), and the outcomes are meticulously presented in Figure 11. Subsequently, this calculated downstream pressure serves as a crucial parameter in determining the pressure ratio, as stipulated by Eq. (3), where the upstream pressure aligns with the ambient pressure. With this pressure ratio established, as graphically depicted in Figure 12, an essential step ensues in discerning the base flow correlation governing the gas mass flow through the orifice (2). This correlation is meticulously illustrated and analyzed in detail, offering valuable insights into the dynamics of gas flow within the system.

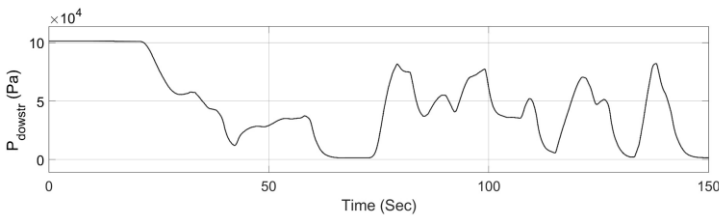


Figure 11. Downstream pressure in the intake manifold

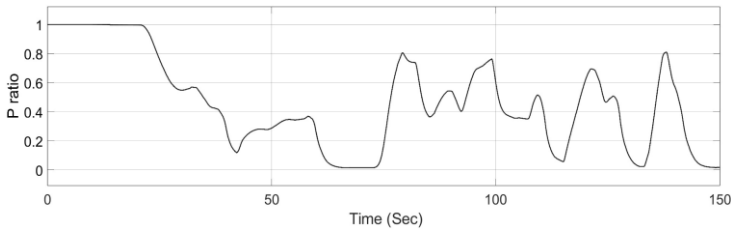


Figure 12. Pressure Ratio

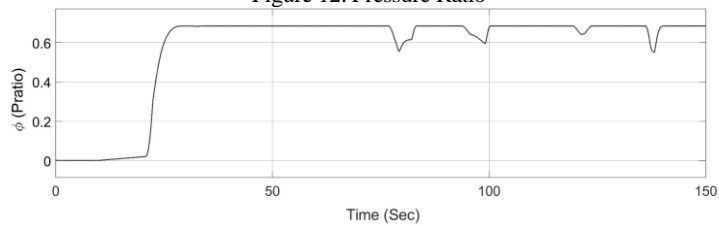


Figure 13. Base flow correlation

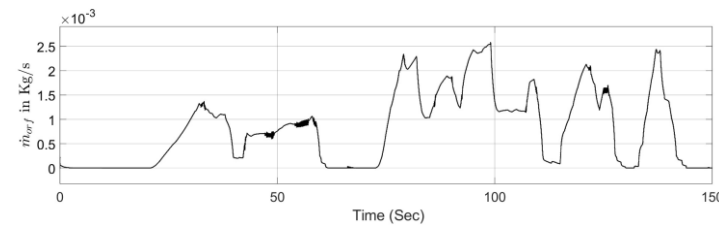


Figure 14. Gas mass flow through the orifice

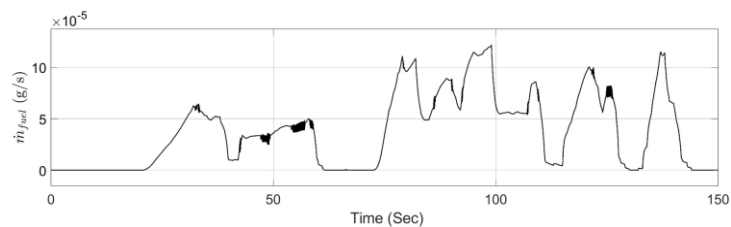


Figure 15. Fuel mass flow rate

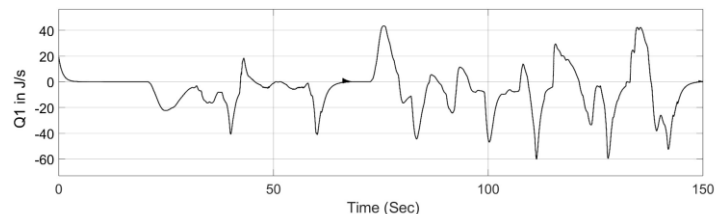


Figure 16. Output heat flow rate

Figures 13 present a comprehensive visualization of this base flow correlation, enriching our understanding of the intricate interplay between pressure differentials and gas mass flow rates as presented in Figure 14. This detailed analysis not only elucidates the fundamental principles governing gas flow behavior but also provides practical

insights crucial for optimizing system performance and efficiency. Within this simulation, hydrogen fuel injection into the intake manifold is implemented, with the corresponding fuel mass flow rate depicted in Figure 15. These parameters play a pivotal role in regulating the combustion process within the engine, ensuring optimal fuel-air mixture ratios and combustion efficiency. By accurately modeling and analyzing the fuel injection dynamics, insights into engine performance, fuel consumption, and emissions can be gleaned. This comprehensive examination of fuel injection characteristics enriches our understanding of engine behavior under varying operating conditions and facilitates the refinement of engine control strategies for enhanced performance and efficiency.

Utilizing the thermal dynamic equations of Eq. (21) to Eq. (27), the heat flow from the internal gas to a specified wall depth, termed as the output heat flow, can be accurately determined. This crucial parameter, which characterizes the heat transfer process within the system, is meticulously presented in Figure 16. Additionally, the heat transfer rate, representing the rate at which heat is exchanged between the gas and the surrounding walls, is quantified based on the same equations and visually depicted in Figure 17.

These analyses offer valuable insights into the thermal dynamics of the system, shedding light on heat distribution, dissipation, and overall thermal performance. By comprehensively understanding the heat transfer processes, engineers can optimize system design, enhance thermal efficiency, and mitigate thermal-related issues, thereby ensuring reliable and efficient operation under diverse operating conditions.

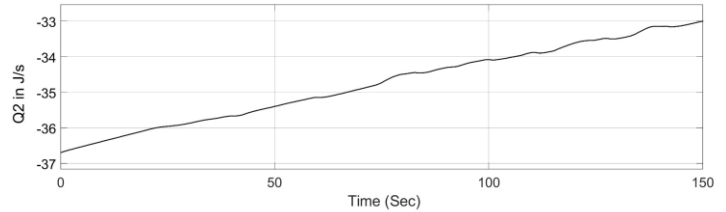


Figure 17. Heat transfer rate

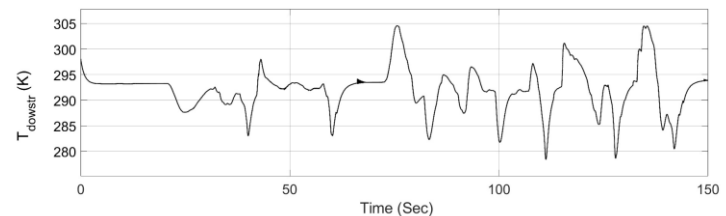


Figure 18. Downstream (intake) temperature

Given the determined output heat flow rate, it becomes feasible to ascertain the intake temperature, also referred to as the downstream temperature, as outlined in Eq. (17). This temperature parameter plays a pivotal role in regulating engine performance and combustion efficiency. By accurately modeling and analyzing the heat transfer dynamics within the system, insights into the variation of intake temperature under different operating conditions can be gained. Figure 18 visually presents these temperature variations, offering a comprehensive understanding of how heat transfer processes influence

intake temperature. This analysis enables engineers to optimize engine operation, ensuring that intake temperatures remain within desired ranges to promote efficient combustion and mitigate potential thermal-related issues.

The mass fraction in the downstream of the intake manifold is determined using Eq. (20), which accounts for various factors influencing the composition of gases within the system. By applying this equation, the simulation yields valuable insights into the downstream mass fraction, representing the proportion of different gas components present in the intake manifold. Figure 19 visually illustrates

the results of this simulation, offering a comprehensive depiction of how the mass fraction varies under different operating conditions. This analysis enhances our understanding of gas composition dynamics within the intake manifold, providing essential information for optimizing combustion processes, controlling emissions, and ensuring efficient engine operation. By closely examining the downstream mass fraction, engineers can make informed decisions regarding fuel-air mixture ratios and combustion strategies, ultimately optimizing engine performance and reducing environmental impact.

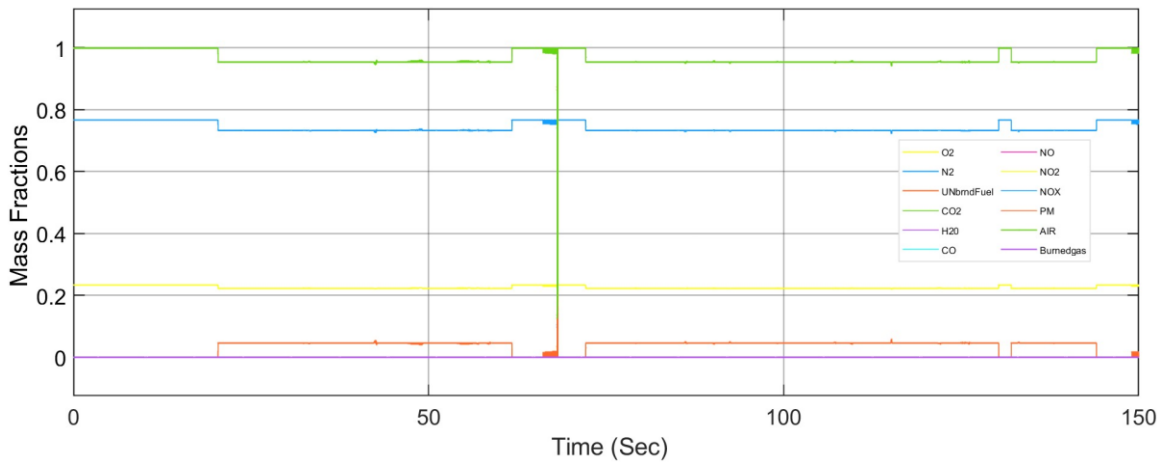


Figure 19. Downstream Mass Fraction

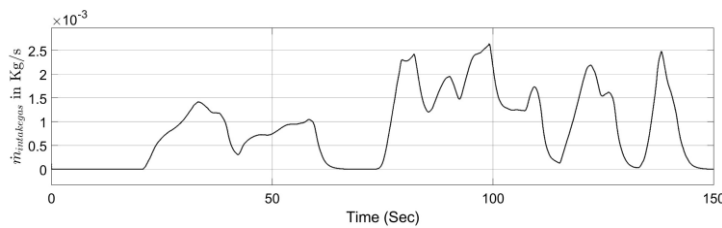


Figure 20. Gas mass flow rate in the chamber

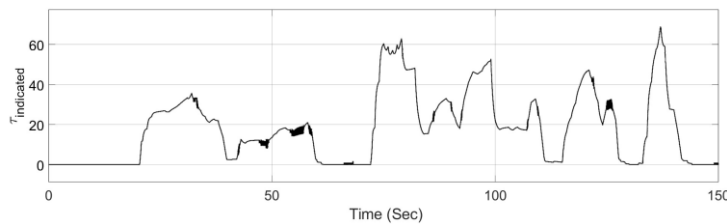


Figure 21. Engine indicated torque

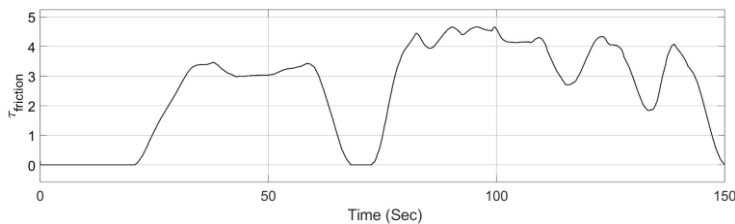


Figure 22. Friction torque

Figure 20 depicts the gas mass flow rate within the chamber, providing crucial insights into the dynamics of gas flow through the engine system. This parameter serves as a fundamental metric for evaluating engine performance and efficiency. Subsequently, utilizing the gas mass flow rate data, the indicated torque can be determined according to Eq. (35), as illustrated in Figure 22. This torque represents the theoretical output torque generated by the engine, reflecting the mechanical power produced during the combustion process. Conversely, Figure 22 presents the friction torque, which accounts for mechanical losses within the engine system.

By comparing the indicated torque with the friction torque, engineers can assess the overall efficiency and mechanical integrity of the engine. Finally, Figure 23 shows the engine speed, providing valuable insights into the rotational speed of the engine's crankshaft under varying operating conditions. Together, these parameters offer a comprehensive understanding of engine performance, enabling engineers to optimize design parameters, refine control strategies, and enhance overall operational efficiency.

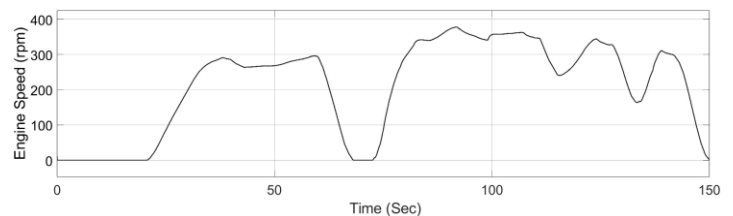


Figure 23. Engine speed

4. Conclusions

In conclusion, this study has centered on the examination of hydrogen's potential as an alternative fuel for proposed hydrogen-powered internal combustion engine (H₂-ICE). Through the adaptation of a dynamic model originally designed for gasoline, a comprehensive dynamic model tailored specifically for ICEs fueled by hydrogen has been successfully developed. This approach underscores the increasing significance of hydrogen as a sustainable energy carrier, presenting a promising pathway towards cleaner transportation solutions. Throughout the simulation results, the effectiveness of the H₂-ICE model was demonstrated using the throttle valve open angle and fuel injector pulse width as references. The model accurately reflected the dynamic behavior of the engine under varying conditions, showcasing its potential for optimizing performance and efficiency. The findings underscore the model's capability to simulate real-world scenarios, providing valuable insights for future research and development in hydrogen-fueled engines. This study highlights the viability of hydrogen as an alternative fuel, contributing to the advancement of sustainable and environmentally friendly automotive technologies. The exploration into the intricate dynamics of hydrogen-powered internal combustion engines contributes substantially to ongoing research and development efforts aimed at advancing cleaner and potentially more efficient automotive technologies. By delving into the operational intricacies of these engines, this study lays the groundwork for future optimization and design endeavors within the realm of hydrogen-powered vehicles. Furthermore, this work not only addresses the pressing need for sustainable energy solutions but also opens up new avenues for innovation and advancement in the field of hydrogen vehicles. Through the successful adaptation and validation of the dynamic model for H₂-ICE, valuable insights into their operational characteristics, efficiency are provided, thus facilitating informed decision-making and strategic planning in the automotive industry.

Acknowledgment

This work was carried out at Altran Prototypes Automobiles (APA) as a part of the Intelligence & Innovation Powertrain project within the Capgemini Engineering Research and Innovation Department.

Nomenclature

T_{abt}	300	Ambient temperature (K)
P_{abt}	101325	Ambient pressure (Pa)
h_{air}		Ambient enthalpy (J/kg)
$c_{p,air}$	1005	Heat coefficient at constant pressure (J/(kgK))
q_{orf}		Heat flow rate (J/s)
h_{upstr}		Upstream specific enthalpy (J/kg)
R	287	Ideal gas constant (J/(kgK))
A_{eff}		Effective cross area
$C_{thr}(\theta_{thr})$		Discharge coefficient
$\theta_{ct,thr}$		Percentage of throttle body that open (%)
γ		Ratio of specific heats
P_{ratio}		Pressure ratio
P_{lim}		Pressure ratio limit
P_{upstr}		Upstream pressure (Pa)
P_{dowstr}		Downstream pressure (Pa)

$y_{upstr,air}$	1	Upstream species air mass fraction
\dot{m}_{orf}		Gas mass flow through the orifice
\dot{m}_{air}		Air mass flow
θ_{thr}		Open angle of the throttle (deg)
D_{thr}		Throttle diameter at opening (m)
Q_1		Heat flow from the internal gas to a specified wall depth (J/s)
$Q_{1,conv}$		Heat flow convection from the internal gas to the internal wall (J/s)
$Q_{1,cond}$		Conduction heat transfer rate (J/s)
Q_2		Heat transfer rate (J/s)
$Q_{2,conv}$		Convection heat transfer (J/s)
$Q_{2,cond}$		Heat flow conduction from the external middle portion of the wall to the external wall (J/s)
T_{intake}		Chamber absolute temperature (K)
P_{intake}		Chamber absolute pressure (Pa)
h_{intake}		Specific enthalpy of the intake manifold (J/kg)
$\dot{m}_{in,intk}$		Chamber input mass flow (kg/s)
$\dot{m}_{out,intk}$		Chamber output mass flow (kg/s)
$q_{in,intk}$		Chamber input heat flow (J/s)
$q_{out,intk}$		Chamber output heat flow (J/s)
$y_{in,intk}$		Input species mass fraction
y_{intake}		Species mass fraction in the chamber
$T_{in,gas}$		Temperature of the gas inside the chamber (K)
$T_{w,int}$		Temperature of the inside wall of the chamber (K)
$T_{ext,gas}$		External gas temperature (K)
$T_{w,ext}$		Temperature of the external wall of the chamber (K)
T_{mass}		Temperature of the thermal mass (K)
k_{int}	25	Thermal conductivity (W/(mK))
$A_{int,cond}$	0.003	Internal conduction area (m ²)
$A_{int,conv}$	0.125	Internal convection area (m ²)
$D_{int,cond}$	0.004	Internal wall thickness (m)
k_{ext}	25	External wall thermal conductivity (W/(mK))
$A_{ext,cond}$	0.003	External conduction area (m ²)
$A_{ext,conv}$	0.125	External convection area (m ²)
$D_{ext,cond}$	0.004	External wall thickness (m)
$c_{q,int}$		Internal convection heat transfer coefficient (W/(m ² K))
$c_{q,ext}$		External convection heat transfer coefficient (W/(m ² K))
$c_{p,wall}$	900	Wall heat capacity (J/(kgK))
m_{wall}	7	Thermal mass (kg)
V_{ch}	29e-4	Chamber volume (m ³)
$ExtnlFlwVel$		External flow velocity
\dot{m}_{fuel}		Fuel mass flow (g/s)
N		Engine speed (rpm)
S_{inj}	6.4516	Fuel injector slope (mg/ms)
$P_{w,nj}$		Fuel injector pulse-width (ms)
N_{cyl}	4	Number of engine cylinders
c_{ps}	2	Crankshaft revolutions per power stroke
$T_{cooling}$		Engine cooling temperature (K)
c_{eng}	40000	Heat capacity
LHV	473e5	Fuel lower heating value (J/kg)
\dot{m}_{fuel}		Fuel mass flow (kg/s)
T_{exh}		Exhaust temperature (K)
τ		Engine brake torque (Nm)
ω		Engine speed (rad/s)

\dot{m}_{intake}		Intake gas mass flow in the chamber (kg/s)
V_d		Displaced volume
L_{eng}		Engine load
η_v		Engine volumetric efficiency
$\eta_{indicated}$		Indicated load efficiency
$\eta_{friction}$		Friction temperature factor
$\tau_{indicated}$		Indicated torque (Nm)
τ_{brake}		Brake torque (Nm)
$\tau_{friction}$		Friction torque (Nm)
ARF		Air fuel ratio
T_{std}	293.15	Standard temperature (K)
P_{std}	101325	Standard pressure (Pa)

Conflict of Interest Statement

Q-T.D and F.H contributed equally. All authors have given approval to the final version of the manuscript. The authors declare that there is no conflict of interest in the study. The authors would also like to thank Guillaume Guilbert who have contributed immensely for the part of the project.

CRediT Author Statement

Fatima Haidar: Writing- review & editing, supervision, project administration & validation. **Quang Truc Dam:** Writing original draft & formal analysis, review & validation. **Nour Mama:** formal analysis & Simulation. **Sherwin Joy Chennapalli:** formal analysis & Simulation

References

- Akal, D., Öztuna, S., & Büyükakın, M. K. (2020). A review of hydrogen usage in internal combustion engines (gasoline-Lpg-diesel) from combustion performance aspect. *International Journal of Hydrogen Energy*, 45(60), 35257–35268.
- Arslan, T. A. (2023). A Comprehensive Review on Stirling Engines. *Engineering Perspective*, 3(3), 42–56.
- Gandhi, R. (2015). Use of Hydrogen in Internal Combustion Engine. *International Journal of Engineering and Technical Research*.
- Knorr, H., Held, W., Prümmer, W., & Rüdiger, H. (1998). The man hydrogen propulsion system for city buses. *International Journal of Hydrogen Energy*, 23(3), 201–208.
- Milojević, S. (2016). Reconstruction of Existing City Buses on Diesel Fuel For Drive on Hydrogen. *Applied Engineering Letters*, 16–23.
- Karagöz, Y. (2017). EFFECT OF HYDROGEN ADDITION AT DIFFERENT LEVELS ON EMISSIONS AND PERFORMANCE OF A DIESEL ENGINE. *Journal of Thermal Engineering*, 1780–1790.
- Stępień, Z. (2021). A Comprehensive Overview of Hydrogen-Fueled Internal Combustion Engines: Achievements and Future Challenges. *Energies*, 14(20), 6504.
- Karakaş, O., Şeker, U. B., & Solmaz, H. (2021). Modeling of an Electric Bus Using MATLAB/Simulink and Determining Cost Saving for a Realistic City Bus Line Driving Cycle. *Engineering Perspective*, 2(2), 52–62.
- Li, X., Zhuang, Y., Wang, Y., Zhu, Z., Qian, Y., & Zhai, R. (2024). An experimental investigation on the lean-burn characteristics of a novel hydrogen fueled spark ignition engine: Hydrogen injection via a micro-hole on the spark plug. *International Journal of Hydrogen Energy*, 57, 990–999.
- Shadidi, B., Najafi, G., & Yusaf, T. (2021). A Review of Hydrogen as a Fuel in Internal Combustion Engines. *Energies*, 14(19), 6209.
- Ehsani, M., Yimin, G., Stefano, L., & Kambiz Ebrahimi, M. (2018). *Modern Electric, Hybrid Electric, and Fuel Cell Vehicles*, Third Edition. CRC Press.
- Singh, A. P., Sharma, N., Agarwal, R., & Agarwal, A. K. (Eds.). (2020). *Advanced Combustion Techniques and Engine Technologies for the Automotive Sector*. Springer Singapore.
- Bayrakçeken, H. (2023). Effect of Clutch Pedal Distances on Fuel Consumption Under Actual Operating Conditions. *Engineering Perspective*, 4(4), 63–67.
- Biswas, S., & Ekoto, I. (2020). Ozone Added Spark Assisted Compression Ignition. In A. P. Singh, N. Sharma, R. Agarwal, & A. K. Agarwal (Eds.), *Advanced Combustion Techniques and Engine Technologies for the Automotive Sector* (pp. 159–185). Springer Singapore.
- Nagareddy, S. (2017). Temperature Distribution Measurement on Combustion Chamber Surface of Diesel Engine -Experimental Method.
- Heywood, J. B. (2018). *Internal combustion engine fundamentals* (Second revised edition). McGraw-Hill Education.
- Kumar, S., Kumar, A., Sharama, A. R., & Kumar, A. (2018). Heat Transfer Correlations on Combustion Chamber Surface of Diesel Engine—Experimental Work. *International Journal of Automotive Science and Technology*, 2(3), 28–35.
- Kumar, S. (2020). Piston Crown Profile Modifications for Various Combustion Mode Strategies of Modified GDI Engine towards NOx and PM Reduction. *International Journal of Automotive Science and Technology*, 4(4), 289–294.
- Nagareddy, S., & Govindasamy, K. (2022b). Influence of fuel system variations on performance and emission characteristics of combined air-wall-guided mode modified GDI engine with alcoholic fuels and exhaust gas recirculation. *Environmental Science and Pollution Research*, 30(22), 61234–61245.
- Nagareddy, S., & Govindasamy, K. (2022a). Combustion chamber geometry and fuel supply system variations on fuel economy and exhaust emissions of GDI engine with EGR. *Thermal Science*, 26(2 Part A), 1207–1217.
- Shivakumar N., Vijayakumar K., Surendran, A., Jose, C., & Mahmood V. K., S. (2023). Impact of blended fuels with split injections on combustion and emission characteristics of spray guided mode modified GDI engine. 020147.
- Nagareddy, S., & Govindasamy, K. (2022). Influence of piston crown shape with different positions of spark plug and fuel injector, %EGR, and fuel system control on emissions from modified GDI engines compared with a base diesel engine. *Transactions of the Canadian Society for Mechanical Engineering*, 46(2), 355–364.
- Falfari, S., Cazzoli, G., Mariani, V., & Bianchi, G. (2023). Hydrogen Application as a Fuel in Internal Combustion Engines. *Energies*, 16(6), 2545.
- Azeem, N., Beatrice, C., Vassallo, A., Pesce, F., Gessaroli, D., Biet, C., & Guido, C. (2024). Experimental study of cycle-by-cycle variations in a spark ignition internal combustion engine fueled with hydrogen. *International Journal of Hydrogen Energy*, 60, 1224–1238.
- Ricci, F., Zembi, J., Avana, M., Grimaldi, C. N., Battistoni, M., & Papi, S. (2024). Analysis of Hydrogen Combustion in a Spark Ignition Research Engine with a Barrier Discharge Igniter. *Energies*, 17(7), 1739.
- Stone, R. (1992). *Introduction to Internal Combustion Engines* (Second edition). The Macmillan Press LTD.